

Cyclometalated Complexes of Ru(II) with 2-Aryl Derivatives of Quinoline and 1,10-Phenanthroline

Céline Bonnefous, Abdellatif Chouai, and Randolph P. Thummel*

Department of Chemistry, University of Houston, Houston, Texas 77204-5003

Received March 14, 2001

Difficulty in cyclometalating 1-(2'-quinolinyl)pyrene and 1,3-di-(2'-quinolinyl)pyrene with Ru(II) led to a more detailed study of the cyclometalation process. A series of 2-aryl-1,10-phenanthrolines, where aryl = phenyl, 2-naphthyl, 1-anthracenyl, and 1-pyrenyl, were treated with [Ru(tpy)Cl₃] to provide either the N5Cl complex [Ru(tpy)(L)Cl]⁺ or this same material as a mixture with the N5C cyclometalated species [Ru(tpy)L]⁺. Steric effects appear to govern the ability of the ligand to attain the near planar conformation required for cyclometalation. The bridged ligand 3,1'-dimethylene-2-(2'-pyrenyl)-1,10-phenanthroline was prepared along with a quinoline analogue. The former species was found to cyclometalate at the C1 of pyrene and afford the N5Cl complex. Both the N5C (*P*₂/*n* (monoclinic), *a* = 28.1102(11), *b* = 8.4638(3), *c* = 31.2908(12) Å, *Z* = 8) and N5Cl (*P*-1 (triclinic), *a* = 11.7235 (10), *b* = 14.5306(12), *c* = 14.5725(12) Å, *Z* = 2) complexes were analyzed by X-ray crystallography, and the N5Cl species evidenced a congested environment for pyrene, which is apparently stabilized by π stacking with tpy. Similar reactions with a series of three 3,2'-bridged derivatives of 2-phenyl-1,10-phenanthroline provide both N5Cl and cyclometalated products in proportions which support the importance of π stacking. The electronic absorption spectra and redox potentials for these complexes evidence strong σ donation by the cyclometalated ligand and an apparent insensitivity to the orthogonal 2-aryl group.

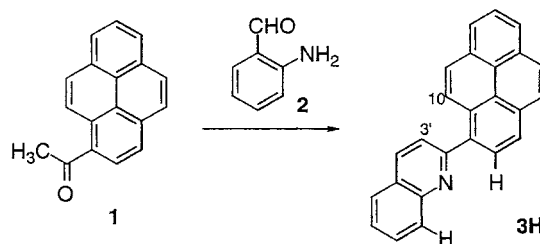
Introduction

The exact manner in which certain chelating ligands, such as 2,2'-bipyridine (bpy) or 2,2',6',2''-terpyridine (tpy), coordinate with d⁶ transition metals is not always well understood. In a recent study, we examined the coordination of a series of tpy analogues with [RuCl₃·3H₂O] and found that, along with formation of the expected hexaaza-coordinated (N₆) species, varying amounts of a pentaaza-coordinated (N₅Cl) complex were formed.¹ Various structural features govern which of these two types of complex is preferred. We also observed that, in some cases, the N₅Cl species could convert to the N₆, and a mechanism was suggested which involved backside displacement of chloride from the metal by the dangling uncomplexed portion of one tpy-type ligand.

If one of the pyridine rings of bpy or tpy is replaced by benzene or another aromatic hydrocarbon, then bidentate or tridentate chelation can only take place, with concurrent cyclometalation of an aryl C–H bond.² Sauvage and co-workers have examined 1,3-di-(2'-pyridyl)-benzene³ and 2,9-di-*p*-tolyl-1,10-phenanthroline,⁴ both of which undergo tridentate chelation with Ru(II) by cyclometalating at a benzene ring. In the latter

case, a relatively long-lived excited state was observed. We thought it might be of interest to incorporate, by cyclometalation to Ru(II), an arene which had more accessible π^* states, and pyrene seemed like an excellent candidate. This paper will discuss our efforts to cyclometalate pyrene and related studies aimed at a better understanding of the cyclometalation process.⁵

Complexation Studies. An initial objective was to prepare a cyclometalated derivative of Ru(II) in which the carbanionic moiety would be part of a pyrene ring. We reasoned that an electro- and photoactive nucleus, such as pyrene, with low lying π^* states would interact in an interesting way if covalently bound to ruthenium. To test this theory we prepared 1-(2'-quinolinyl)pyrene (**3H**) by the Friedländer condensation of 2-aminobenzaldehyde (**2**) with 1-acetylpyrene (**1**).⁶ Treatment of this ligand with [Ru(bpy)₂Cl₂] in refluxing aqueous ethanol led only to recovery of the starting materials.



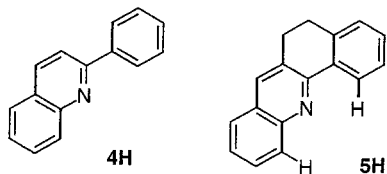
We reasoned that in the planar conformation of **3H** required for cyclometalation at C2, there would be an unfavorable

* To whom correspondence should be addressed.

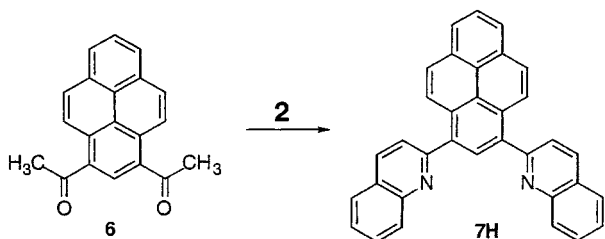
- (1) Jahng, Y.; Thummel, R. P.; Bott, S. G. *Inorg. Chem.* **1997**, *36*, 3133.
- (2) (a) Constable, E. C.; Rees, D. G. F. *New J. Chem.* **1997**, *21*, 369. (b) Constable, E. C.; Dunne, S. J.; Rees, D. G. F.; Schmitt, C. X. *J. Chem. Soc., Chem. Commun.* **1996**, 1169. (c) Constable, E. C.; Thompson, A. M. W. C. *New J. Chem.* **1996**, *20*, 65. (d) Constable, E. C.; Thompson, A. M. W. C.; Cherryman, J.; Liddiment, T. *Inorg. Chim. Acta* **1995**, *235*, 165. (e) Constable, E. C.; Thompson, A. M. W. C.; Greulich, S. *J. Chem. Soc., Chem. Commun.* **1993**, 1444. (f) Constable, E. C.; Hannon, M. J. *Inorg. Chim. Acta* **1993**, *211*, 101. (g) Constable, E. C.; Henney, R. P. G.; Tocher, D. A. *J. Chem. Soc., Dalton Trans.* **1992**, 2467. (h) Constable, E. C.; Henney, R. P. G.; Tocher, D. A. *J. Chem. Soc., Dalton Trans.* **1991**, 2335. (i) Constable, E. C.; Henney, R. P. G.; Leese, T. A.; Tocher, D. A. *J. Chem. Soc., Dalton Trans.* **1990**, 443. (j) Constable, E. C.; Holmes, J. M. *J. Organomet. Chem.* **1986**, *301*, 203. (k) Constable, E. C. *Polyhedron* **1984**, *3*, 1037.

- (3) Barigelletti, F.; Flamigni, L.; Massimo, G.; Juris, A.; Beley, M.; Chodorowski-Kimines, S.; Collin, J.-P.; Sauvage, J.-P. *Inorg. Chem.* **1996**, *35*, 136. (b) Beley, M.; Chodorowski, S.; Collin, J.-P.; Sauvage, J.-P.; Flamigni, L.; Barigelletti, F. *Inorg. Chem.* **1994**, *33*, 2544. (c) Beley, M.; Collin, J.-P.; Sauvage, J.-P. *Inorg. Chem.* **1993**, *32*, 4539. (d) Beley, M.; Chodorowski, S.; Collin, J.-P.; Sauvage, J.-P. *Tetrahedron Lett.* **1993**, *34*, 2933. (e) Beley, M.; Collin, J.-P.; Louis, R.; Metz, B.; Sauvage, J.-P. *J. Am. Chem. Soc.* **1991**, *113*, 8521.

interaction between H10 on pyrene and H3' on quinoline. To assess the importance of this effect, 2-phenylquinoline (**4H**) was examined and also found to be unreactive when refluxed in aqueous ethanol with $[\text{Ru}(\text{bpy})_2\text{Cl}_2]$. Conformational mobility about the (2-1')-bond in **4H** could also be a problem, so we examined the dimethylene bridged analogue **5H**, where a two carbon bridge holds the molecule approximately planar.⁷ Again, cyclometalation was not observed. Both reactions were also unsuccessful using Ag(I) to activate the reagent in a manner similar to that employed by Constable and Holmes for the cyclometalation of 2-phenylpyridine.^{2j} Considering that the initial step in the desired process would be N–Ru complexation, the interference of both the C2 phenyl group and quinoline H8 apparently prevent this crucial first step.

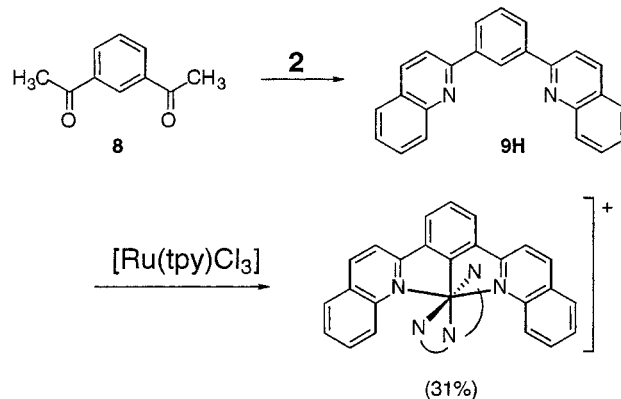


To help overcome this reluctance to cyclometalate, we next investigated systems which were more analogous to those studied by Sauvage. If the pyrene were part of a potential tridentate chelator, the chance for inducing cyclometalation might improve. The condensation of 2 equiv of 2-aminobenzaldehyde with 1,3-diacetylpyrene (**6**)⁸ provided 1,3-di-(2'-quinolinyl)pyrene (**7H**) in 72% yield. Attempted complexation with $[\text{Ru}(\text{tpy})\text{Cl}_3]$ was unsuccessful, and unreacted starting materials were recovered. The same result was obtained when the complexation protocol of Sauvage was followed, wherein the $[\text{Ru}(\text{tpy})\text{Cl}_3]$ was first activated by solvolysis with AgClO_4 in acetone.^{3e}

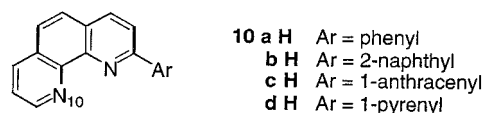


When 1,3-diacetylbenzene was substituted for **6**, the ligand 1,3-di-(2'-quinolinyl)benzene (**9H**) could be prepared in 56% yield, and this species did form a cyclometalated complex with $[\text{Ru}(\text{tpy})\text{Cl}_3]$. This result was somewhat surprising in that the kinetic acidity of pyrene is considerably greater than that of benzene.⁹ These observations led us to more carefully consider the discrete steps involved in the formation of complexes such as $[\text{Ru}(\text{tpy})(\mathbf{9})]^+$. After the initial coordination of a quinoline nitrogen of either **3H** or **7H** with ruthenium, the pyrene must then oxidatively add to the metal center. The third coordinative

bond, which helps to stabilize the system, would most likely form only after the cyclometalation step had occurred. It is interesting that **9H** will undergo the prerequisite initial N–Ru coordination even though the ligand is more sterically encumbered than **4H**, which does not cyclometalate. The difference may be explained by comparing attack on $[\text{Ru}(\text{bpy})_2\text{Cl}_2]$ with $[\text{Ru}(\text{tpy})\text{Cl}_3]$, where the latter species is more sterically accessible. It is noteworthy that the oxidation state of ruthenium differs for these two reagents. One could argue that Ru(III) is more electrophilic and, hence, more reactive in the first complexation step. Reduction of the metal (accompanied by solvent oxidation) occurs during the stepwise coordination, probably after complexation of the first pyridine.



To probe the cyclometalating ability of increasingly delocalized aromatic systems, we next examined the series of ligands **10a–dH**, which had been prepared in earlier work.¹⁰ These ligands are all 2-aryl derivatives of 1,10-phenanthroline (phen) where cyclometalation at an ortho position of the 2-aryl ring is expected to lead to an NNC complex. It was anticipated that initial bidentate coordination to the phen portion of the ligand would facilitate the cyclometalation step.



- 10 a H** Ar = phenyl
b H Ar = 2-naphthyl
c H Ar = 1-anthracenyl
d H Ar = 1-pyrenyl

The reagent $[\text{Ru}(\text{tpy})\text{Cl}_3]$ consists of a tpy, one chloride bound in the equatorial plane, and two axial chlorides. When 2-phenylphen (**10aH**) was treated with $[\text{Ru}(\text{tpy})\text{Cl}_3]$ a mixture of two products was formed. The formation of these products might depend on whether initial attack of the more sterically accessible phen N10 occurred to replace an axial or equatorial chloride. In the case of axial attack, the NNC cyclometalated complex $[\text{Ru}(\text{tpy})(\mathbf{10a})]^+$ was formed in 35% yield. If initial attack occurs to replace an equatorial chloride, the N5Cl complex $[\text{Ru}(\text{tpy})(\mathbf{10aH})\text{Cl}]^+$ is formed in 12% yield. The two complexes are readily characterized by several diagnostic ¹H NMR resonances.^{2f,11} For $[\text{Ru}(\text{tpy})(\mathbf{10a})]^+$, H3', which is adjacent to the cyclometalated C2' carbon, is highly shielded and, therefore, shifted upfield, appearing as a doublet at 5.79 ppm. For the N5Cl complex $[\text{Ru}(\text{tpy})(\mathbf{10aH})\text{Cl}]^+$, the ortho protons on the phenyl ring (H2' and H6') are shielded and appear as a doublet at 6.11 ppm. This shielding is due both to the tpy ring, which lies parallel to the phenyl ring, and the phen ring, which is orthogonal, causing H2' and H6' to lie partially above and below

(4) Collin, J.-P.; Kayhanian, R.; Sauvage, J.-P.; Calogero, G.; Barigelletti, F.; De Cian, A.; Fischer, J. *J. Chem. Soc., Chem. Commun.* **1997**, 775.

(5) Bruce, M. I. *Angew. Chem., Int. Ed. Engl.* **1977**, *16*, 73.

(6) (a) Thummel, R. P. *Synlett.* **1992**, *1*. (b) Cheng, C.-C.; Yan, S.-J. *Org. React.* **1982**, *28*, 37.

(7) Thummel, R. P.; Decloitre, Y.; Lefoulon, F. *J. Heterocycl. Chem.* **1986**, *23*, 689.

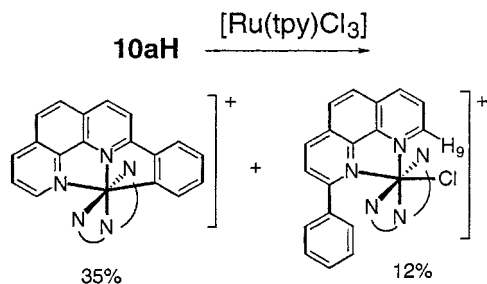
(8) (a) Scott, L. T.; Nacula, A. *J. Org. Chem.* **1996**, *61*, 386. (b) Harvey, R. G.; Pataki, J.; Lee, H. *Org. Prep. Proced. Int.* **1984**, *16*, 144.

(9) Cram, D. J. *Fundamentals of Carbanion Chemistry*; Academic Press: New York, 1965; p 26.

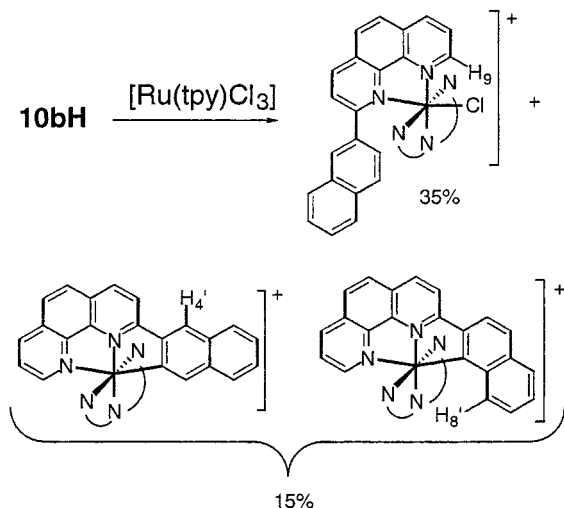
(10) Riesgo, E. C.; Jin, X.; Thummel, R. P. *J. Org. Chem.* **1996**, *61*, 3017.

(11) Reveco, P.; Medley, J. H.; Garber, A. R.; Bhacca, N. S.; Selbin, J. *Inorg. Chem.* **1985**, *24*, 1096.

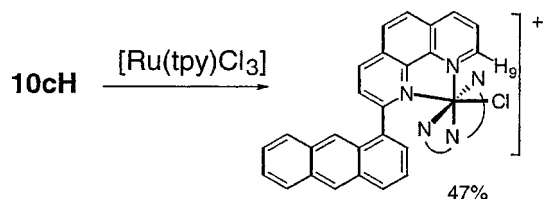
its shielding face. Even more characteristic is H9 which is strongly deshielded by the proximal chloride and appears as a doublet at 10.46 ppm. Due to the presence of a number of independent spin systems, it was often possible to make complete proton assignments by careful analysis of the 2D ^1H NMR.



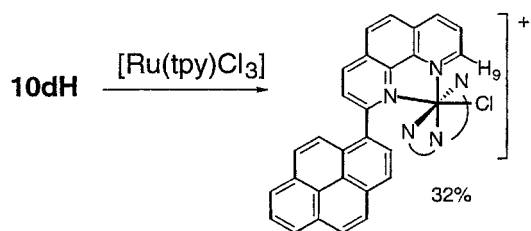
When the 2-(2'-naphthyl) derivative **10bH** is treated with $[\text{Ru}(\text{tpy})\text{Cl}_3]$, three products are formed, but now the noncyclometalated product predominates and is afforded in 35% yield. It is again identified by the H9 resonance at 10.47 ppm. In the upfield region we observe the protons ortho to the C2-phen bond, a doublet for H3' at 6.26 ppm, and a singlet for H1' at 6.52 ppm. A mixture of two cyclometalated products were formed in a 4/1 ratio, and this mixture could not be separated. The major product was bound to ruthenium at C2', giving rise to a singlet at 6.15 ppm for H4'. The minor product was bound to ruthenium at C1', giving rise to a doublet at 6.42 ppm for H8'.



With the 1-anthracenyl derivative **10cH**, a 47% yield of only the N5Cl product $[\text{Ru}(\text{tpy})(\text{10cH})\text{Cl}]^+$ is obtained. It is characterized by the highly deshielded H9 resonance at 10.44 ppm and a shielded doublet for H2' at 5.92 ppm.

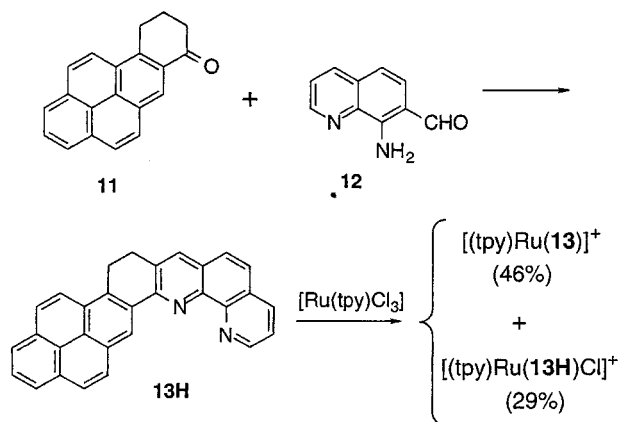


A similar result is obtained for the 1-pyrenyl derivative **10dH**, which provides a 32% yield of the N5Cl product $[\text{Ru}(\text{tpy})(\text{10dH})\text{Cl}]^+$ characterized by the highly deshielded H9 resonance at 10.43 ppm and a shielded doublet for H2' at 6.53 ppm.

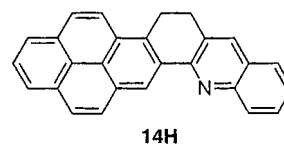


For **10cH** and **10dH**, the course of the reaction appears to be dictated by the conformation of the pendant 2-aryl group. In both cases the planar conformation required for cyclometalation to give a five-membered chelate ring would involve an unfavorable interaction between H3 on phen and a proton on the aryl substituent. This interaction is avoided when the aryl group lies orthogonal to the plane of the phen ring, and in this conformation, a favorable π stacking effect is also evident between the aryl group and the incoming tpy.

To hold a 2-pyrenyl group more coplanar to the phen and avoid the unfavorable H,H interaction, we next chose to examine ligand **13H**, which could be prepared in 90% yield by the condensation of 9,10-dihydrobenzo[*a*]pyren-7(8H)-one (**11**) with 8-amino-7-quinolinecarbaldehyde (**12**).¹⁰ In this instance, the cyclometalated N5C complex $[(\text{tpy})\text{Ru}(\text{13H})]^+$ was obtained in 46% yield along with 29% of the N5Cl complex $[(\text{tpy})\text{Ru}(\text{13H})\text{Cl}]^+$. It is noteworthy that the C1 of pyrene is considerably more reactive toward electrophiles than C2. This reactivity difference may also play an important role in the results obtained for **13H** versus **10dH**.



The successful tridentate cyclometalation of **13H** raised the question of whether a similar bidentate reaction might be possible utilizing C1 and a bridged analogue of **3H**. Thus, ligand **14H** was prepared in 84% yield by the reaction of **11** with **2**. Treating **14H** with $[\text{Ru}(\text{bpy})_2\text{Cl}_2]$ under normal conditions (refluxing aqueous ethanol), using AgBF_4 , or even in a microwave reactor (glycerol), led only to recovered ligand.

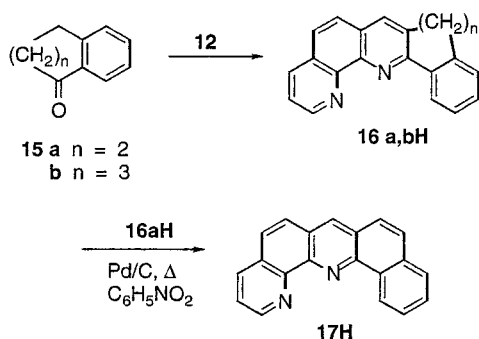


In an earlier study, we observed that exposure of the N5Cl product, $[\text{Ru}(\text{tpy})_2\text{Cl}]^+$, to ambient light resulted in a smooth conversion to the fully coordinated N6 species by what appeared to be a backside displacement of chloride by the uncomplexed nitrogen.¹ A similar experiment using $[\text{Ru}(\text{tpy})(\text{10aH})\text{Cl}]^+$ did

not evidence any change due to the weak nucleophilicity of benzene as compared to pyridine.

An important factor in determining the precoordination geometry leading to N5Cl complexation is the degree of flexibility about the bond joining the aryl substituent to the phen ring. The more orthogonal these two rings are to one another, the more easily the phen ring is able to coordinate. Furthermore, an orthogonal 2-aryl ring may π stack with the incoming tpy, thus providing a favorable precoordination geometry. To probe this effect, a series of bridged derivatives of 2-phenylphen (10aH) was prepared.

The Friedländer condensation of 8-amino-7-quinolinecarbaldehyde (12) with 1-tetralone (15a) or benzosuberone (15b) led to the dimethylene and trimethylene bridged derivatives 16a,bH in yields of 82% and 52%, respectively. The dimethylene species 16aH could be dehydrogenated in 59% yield by heating with palladium on carbon in nitrobenzene for 2 days. Molecular mechanics calculations were used to determine the approximate geometry of an energy minimized form of these three ligands; particular attention was paid to the dihedral angle about the 2,2'-bond.¹² For 16aH, this angle was estimated to be 17°, for 16bH it was estimated at 44°, and 17H was found to be approximately planar. These three ligands were then complexed with [Ru(tpy)-Cl₃] with quite different results.



For 16bH, which showed the greatest degree of twist about the 2,2'-bond, π stacking of the 2-phenyl substituent with the tpy of the reagent would displace the phen moiety in a manner reasonably favorable to initial complexation of N1 in the equatorial plane of [Ru(tpy)Cl₃], and thus, 34% [Ru(tpy)(16bH)-Cl]⁺ was obtained, as compared to only 6% of the cyclometalated complex [Ru(tpy)(16b)]⁺. For 16aH, the ligand is more planar and thus less able to adopt a conformation favorable to precoordination π stacking. Nevertheless, formation of the N5Cl species [Ru(tpy)(16aH)Cl]⁺ still accounts for 48% of the product, while 40% of cyclometalated [Ru(tpy)(16a)]⁺ is also obtained. For 17H, the ligand is essentially planar, and only the cyclometalated species [Ru(tpy)(17)]⁺ is observed in 57% yield.

Properties of the Complexes. The distinctly different complexation results obtained for 10dH and 13H prompted us to more closely examine the structural properties of the two complexes derived from the latter species. Figure 1 illustrates the ORTEP drawing of the cation associated with the cyclometalated species [Ru(tpy)(13)](PF₆), and Table 1 summarizes some of the important geometric features of this complex. The two ligands are oriented in approximately orthogonal planes as one would expect for normal bis-tridentate octahedral coordination. The Ru–C21 bond to pyrene is slightly shorter than the opposing Ru–N1 bond, reflecting the stronger σ donor ability

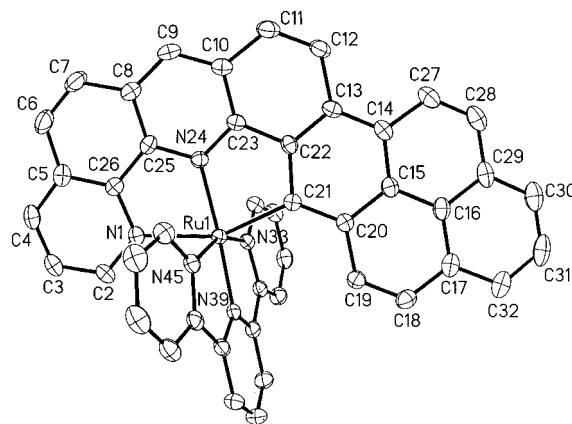


Figure 1. ORTEP drawing of the cation of [Ru(tpy)(13)](PF₆) with atomic numbering scheme.

Table 1. Selected Bond Lengths, Bond Angles, and Dihedral Angles for [Ru(13)(tpy)](PF₆) and [Ru(13H)(tpy-*d*₁₁)Cl](PF₆)^a

[Ru(13)(tpy)](PF ₆)		[Ru(13H)(tpy- <i>d</i> ₁₁)Cl](PF ₆)	
Bond Lengths (Å)			
Ru–N1	2.188(3)	Ru–N1	2.074(5)
Ru–N24	2.007(3)	Ru–N24	2.135(4)
Ru–C21	2.091(3)	Ru–Cl	2.3767(14)
Ru–N33	2.063(3)	Ru–N33	2.080(4)
Ru–N39	1.959(3)	Ru–N39	1.954(4)
Ru–N45	2.064(3)	Ru–N45	2.057(4)
Bond Angles (°)			
N1–Ru–N24	76.68(10)	N1–Ru–N24	79.33(17)
N24–Ru–C21	78.68(11)	N24–Ru–Cl	166.16(11)
N33–Ru–N39	78.94(10)	N33–Ru–N39	78.89(17)
N39–Ru–N45	79.24(11)	N39–Ru–N45	79.75(17)
N24–Ru–N39	176.03(11)		
Dihedral Angles (°)			
N33–C38–C40–N39	–0.8(4)	N33–C38–C40–N39	–5.3(7)
C37–C38–C40–C41	0.7(6)	C37–C38–C40–C41	–8.3(9)
N39–C44–C46–N45	–5.0(4)	N39–C44–C46–N45	–0.2(7)
C43–C44–C46–C47	–9.1(6)	C43–C44–C46–C47	1.4(9)
C21–C22–C23–N24	–10.1(4)	C21–C22–C23–N24	–34.3(7)
C13–C22–C23–C10	–15.5(5)	C13–C22–C23–C10	–31.8(6)

^a Numbering pattern from Figures 1 and 2 with esd's in parentheses.

of the anionic carbon. This causes the N1–Ru–N24 angle to be about 2° less than the N24–Ru–C21 angle, pushing C19 toward the central pyridine of the tpy ligand. The attached proton (H4') is therefore strongly shielded and appears as the highest field aromatic resonance in the ¹H NMR (doublet at 6.46 ppm). The degree of twist between the phen and pyrene rings can be estimated as 12.8°, the average of the two dihedral angles containing C22 and C23. This twist relieves eclipsing interactions in the dimethylene bridge while allowing efficient tridentate complexation.

A suitable crystal of the N5Cl complex was obtained from an experiment in which tpy-*d*₁₁ was substituted for tpy. The situation for this complex is more interesting in that two binding modes are possible for the phen ligand, with N1 either occupying a site in the equatorial plane of the tpy ligand or the axial site orthogonal to this plane. Steric considerations appeared to favor N1 being axial so as to position tpy away from the bulky pyrene residue. The ¹H NMR spectrum for the complex showed a highly deshielded doublet for H9 (attached to C2 in Figure 2) appearing at 10.28 ppm. The small coupling constant of 5.3 Hz is diagnostic of H9, and the deshielding is due to the proximal chlorine. The X-ray structure supports the NMR assignment, showing the tpy to be close to the pyrene moiety. A similar

(12) Calculations were performed with the program PC MODEL available from Serena Software, Bloomington, IN.

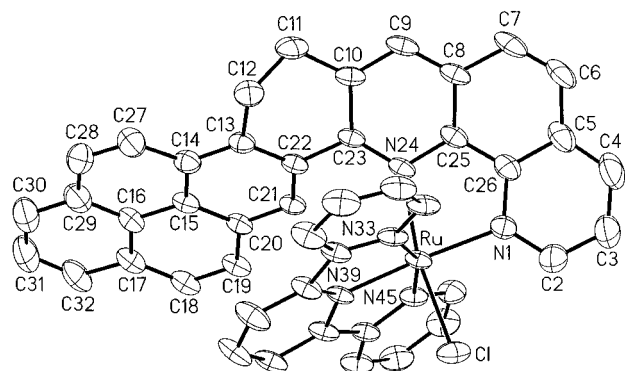


Figure 2. ORTEP drawing of the cation of $[\text{Ru}(\text{tpy})(\mathbf{13H})\text{Cl}](\text{PF}_6)$ with atomic numbering scheme.

orientation was observed in an N5Cl complex reported earlier.¹ Compared with the cyclometalated complex, the Ru–N1 bond shortens and the Ru–N24 bond lengthens, reflecting some steric congestion between the two organic ligands. The dihedral angle between the phen and pyrene rings has increased to about 33°, and there appears to be a π – π interaction between the benzo ring bonded to phen and the central pyridine of tpy. The distance between the centers of these two rings is 3.63 Å, and the dihedral angle between their mean planes is 30.8°.

The seven N5Cl complexes which have been characterized in this study show resonances for H9 in the range of 10.20–10.46 ppm, indicating that they all have a geometry similar to $[\text{Ru}(\text{tpy})(\mathbf{13H})\text{Cl}](\text{PF}_6)$. This consistency allows us to analyze the complexation process leading to this geometry. Ligands **10cH** and **10dH** have larger π surfaces and the freedom to orient the 2-aryl ring orthogonal to the phen. The π stacking of this 2-aryl ring with the tpy of the incoming Ru(II) reagent would favor the observed geometry. Systems where this π surface is smaller (**10aH**) or where a dimethylene bridge may enforce planarity of the ligand thereby inhibiting effective π stacking (**13H** or **16aH**) may lead to increased amounts of cyclometalated products.

The electronic absorption data for the ligands and their Ru(II) complexes are summarized in Table 2. An interesting trend can be noted for the three bridged ligands. As the bridge lengthens in going from **16aH** to **16bH**, the degree of conjugation between the 2-phenyl substituent and the phen is diminished, resulting in a shift of the absorption maximum to higher energy.⁷ For **17H**, the absorption maximum appears at considerably longer wavelength (387 nm) due to the more delocalized π system of this fully conjugated molecule.

The two classes of Ru(II) complexes show distinct properties in their electronic absorption spectra. The seven N5Cl complexes show a long wavelength maximum in the range of 500–511 nm. This absorption is attributed to the typical metal-to-ligand charge transfer (MLCT) that is characteristic of most Ru(II) polypyridine complexes.¹³ The MLCT band for $[\text{Ru}(\text{tpy})_2]^{2+}$ in acetonitrile appears at 474 nm. An approximate 30 nm shift to lower energy for the N5Cl complexes may be explained by destabilization of the metal t_{2g} orbital, which is caused by the chloride being a stronger π donor than the pyridine ligand. It is quite interesting that the increasing conjugation and electron delocalizing ability of the 2-aryl substituent along the series **10a–dH** makes essentially no difference in the absorption

Table 2. Electronic Absorption Maxima (nm) and Molar Absorptivities ($\log \epsilon$) for the Ligands and Their Ru(II) Complexes^a

compound	λ_{max} ($\log \epsilon$)
10aH	351 (3.69), 285 (4.76), 234 (4.89)
$[\text{Ru}(\text{tpy})(\mathbf{10aH})\text{Cl}]^+$	512 (4.17), 316 (4.65), 303 (4.66), 277 (4.75), 233 (4.84)
$[\text{Ru}(\text{tpy})(\mathbf{10aH})\text{Cl}]^+$	500 (4.05), 320 (4.45), 269 (4.71), 227 (4.73)
10bH	276 (4.55), 237 (4.73), 215 (4.56)
$[\text{Ru}(\text{tpy})(\mathbf{10bH})\text{Cl}]^+$	515 (4.16), 305 (4.68), 275 (4.65), 233 (4.78), 199 (4.82)
$[\text{Ru}(\text{tpy})(\mathbf{10bH})\text{Cl}]^+$	501 (4.03), 317 (4.46), 269 (4.78), 222 (4.94)
10cH	380 (3.95), 252 (5.02), 230 (4.81)
$[\text{Ru}(\text{tpy})(\mathbf{10cH})\text{Cl}]^+$	503 (4.01), 321 (4.38), 270 (4.83), 251 (4.88), 238 (4.88), 201 (4.77)
10dH	342 (4.44), 277 (4.67), 233 (4.94), 195 (4.80)
$[\text{Ru}(\text{tpy})(\mathbf{10dH})\text{Cl}]^+$	502 (4.02), 321 (4.63), 270 (4.89), 238 (4.95)
13H	394 (4.11), 358 (4.39), 343 (4.62), 306 (4.69), 242 (4.59)
$[\text{Ru}(\text{tpy})(\mathbf{13H})\text{Cl}]^+$	514 (4.19), 464 (4.04), 395 (4.39), 319 (4.75), 235 (4.71)
$[\text{Ru}(\text{tpy})(\mathbf{13H})\text{Cl}]^+$	511 (3.81), 315 (4.53), 277 (4.47), 238 (4.59)
16aH	356 (4.06), 339 (4.06), 293 (4.48), 238 (4.68), 192 (4.37)
$[\text{Ru}(\text{tpy})(\mathbf{16aH})\text{Cl}]^+$	511 (4.19), 303 (4.58), 277 (4.58), 236 (4.72), 195 (4.76)
$[\text{Ru}(\text{tpy})(\mathbf{16aH})\text{Cl}]^+$	506 (3.96), 317 (4.50), 281 (4.51), 233 (4.69)
16bH	345 (3.51), 329 (3.68), 280 (4.57), 237 (4.73)
$[\text{Ru}(\text{tpy})(\mathbf{16bH})\text{Cl}]^+$	517 (4.18), 305 (4.56), 277 (4.58), 237 (4.69), 194 (4.68)
$[\text{Ru}(\text{tpy})(\mathbf{16bH})\text{Cl}]^+$	500 (3.99), 321 (4.43), 276 (4.63), 232 (4.70)
17H	387 (3.71), 366 (3.72), 294 (4.71), 240 (4.39), 222 (4.58)
$[\text{Ru}(\text{tpy})(\mathbf{17H})\text{Cl}]^+$	553 (4.20), 369 (4.22), 316 (4.68), 276 (4.66), 236 (4.75)

^a Measured in CH_3CN (10^{-5} M).

spectra, and all four systems show nearly the same MLCT transition. The implication is that the 2-substituent, being orthogonal to the phen, is electronically decoupled from the system and plays essentially no role. It is attractive to suggest that interligand communication might occur through π stacking with the tpy, but the electronic spectra offer no support of this premise. We have observed a similar decoupling of states for the complex $[\text{Ru}(\text{bpy})_2(\mathbf{10dH})]^{2+}$.¹⁴ The N5Cl complexes also show a weak, low energy absorption at about 640 nm (Figure 3). We found this identical absorption in the parent system $[\text{Ru}(\text{phen})(\text{tpy})\text{Cl}]^+$, and it appears to be characteristic of N5Cl chlororuthenium(II) complexes.

For the cyclometalated series, the σ donating effect is more pronounced, and the absorption maximum of the MLCT band shifts to 511–517 nm and is somewhat more intense. For these N5C coordinated systems, the carbanionic ligand is even a stronger donor than pyridine, leading to greater destabilization of the ruthenium(II).¹⁵ The complex $[\text{Ru}(\text{tpy})(\mathbf{17H})\text{Cl}]^+$ exhibits the lowest energy transition with a maximum at 553 nm (Figure 3) due to the extensive delocalization provided by the fully conjugated **17** and the consequent lowering of the π^* state for this system.

Figure 3 also illustrates the situation for the N5Cl and cyclometalated complexes of **16a,bH** and **17H**. Despite their relatively different conformations, the spectra for both types of **16a,bH** complex are remarkably similar, indicating again the relative unimportance of the 2-aryl substituent. When excited

(13) (a) Kalyanasundaram, K. *Photochemistry of Polypyridine and Porphyrin Complexes*; Academic Press: San Diego, 1992. (b) Juris, A.; Balzani, V.; Barigelli, F.; Campagna, S.; Belsler, P.; von Zelewsky, A. *Coord. Chem. Rev.* **1988**, *84*, 85.

(14) Simon, J. A.; Curry, S. L.; Schmehl, R. H.; Schatz, T. R.; Piotrowiak, P.; Jin, X.; Thummel, R. P. *J. Am. Chem. Soc.* **1997**, *119*, 11012.

(15) (a) Reveco, P.; Cherry, W. R.; Medley, J.; Garber, A.; Gale, R. J.; Selbin, J. *Inorg. Chem.* **1986**, *25*, 1842. (b) Reveco, P.; Schmehl, R. H.; Cherry, W. R.; Fronczek, F. R.; Selbin, J. *Inorg. Chem.* **1985**, *24*, 4078.

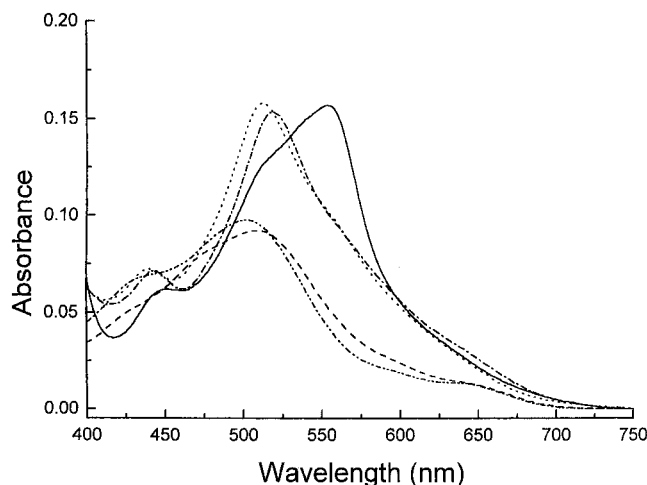


Figure 3. Long wavelength region of the electronic absorption spectra of Ru(II) complexes, 10^{-5} M in CH_3CN : $[\text{Ru}(\text{tpy})(\mathbf{16a})]^+$ (dotted), $[\text{Ru}(\text{tpy})(\mathbf{16aH})\text{Cl}]^+$ (dashed), $[\text{Ru}(\text{tpy})(\mathbf{16b})]^+$ (dash-dot), $[\text{Ru}(\text{tpy})(\mathbf{16bH})\text{Cl}]^+$ (dash-dot-dot), and $[\text{Ru}(\text{tpy})(\mathbf{17})]^+$ (solid).

Table 3. Half Wave Oxidation and Reduction Potentials (V versus SCE) for the Ru(II) Complexes^a

complex	$E_{1/2}$ (ox)	$E_{1/2}$ (red)
$[\text{Ru}(\text{tpy})(\mathbf{10a})]^+$	0.58 (90), 1.27 (100)	-1.58 (90), -1.86 (90)
$[\text{Ru}(\text{tpy})(\mathbf{10aH})\text{Cl}]^+$	0.81 (80)	-1.46 (100)
$[\text{Ru}(\text{tpy})(\mathbf{10b})]^+$	0.58 (80), 1.36 (100)	-1.49 (90)
$[\text{Ru}(\text{tpy})(\mathbf{10bH})\text{Cl}]^+$	0.81 (90)	-1.37 (90), -1.80 (90)
$[\text{Ru}(\text{tpy})(\mathbf{10cH})\text{Cl}]^+$	0.83 (100)	-1.52 (60), -1.85 (irr) ^b
$[\text{Ru}(\text{tpy})(\mathbf{10dH})\text{Cl}]^+$	0.84 (100)	-1.59 (100), -1.86 (irr)
$[\text{Ru}(\text{tpy})(\mathbf{13})]^+$	0.57 (100), 1.13 (160)	-1.51 (90), -1.82 (150)
$[\text{Ru}(\text{tpy})(\mathbf{13H})\text{Cl}]^+$	0.84 (90)	-1.57 (85), -1.86 (irr)
$[\text{Ru}(\text{tpy})(\mathbf{16a})]^+$	0.60 (80), 1.33 (100)	-1.57 (80), -1.89 (110)
$[\text{Ru}(\text{tpy})(\mathbf{16aH})\text{Cl}]^+$	0.83 (90)	-1.43 (70), -1.76 (80)
$[\text{Ru}(\text{tpy})(\mathbf{16b})]^+$	0.54 (80), 1.19 (120)	-1.58 (80), -1.89 (110)
$[\text{Ru}(\text{tpy})(\mathbf{16bH})\text{Cl}]^+$	0.80 (90)	-1.51 (80)
$[\text{Ru}(\text{tpy})(\mathbf{17})]^+$	0.62 (90), 1.34 (irr)	-1.33 (90)

^a Solutions were 0.1 M TBAP in CH_3CN ; the sweep rate was 200 mV/s; the number in parentheses is the difference (mV) between the anodic and cathodic waves. ^b Irr = irreversible.

at the wavelength of their MLCT absorption, none of the complexes studied showed appreciable luminescence at room temperature.

The half wave oxidation and reduction data for the Ru(II) complexes, as determined by cyclic voltammetry, are summarized in Table 3. Again there is a strong consistency of the data. Oxidations of the N5Cl complexes all occur in the range of +0.80 to +0.84 V, which is substantially less than the potential of +1.27 V¹⁶ observed for $[\text{Ru}(\text{tpy})_2]^{2+}$. Since oxidation of complexes of this type are known to be metal based,¹³ it is the better π donor ability of chloride as compared to pyridine which raises the energy of the ruthenium t_{2g} orbital and thus diminishes the energy required for oxidation. The σ donor effect is stronger for the carbanionic cyclometalated complexes, where now the range of oxidation potentials is still lower, +0.54 to +0.62 V. Insensitivity to the ligand is illustrated by $[\text{Ru}(\text{tpy})(\mathbf{17})]^+$ which, despite the more delocalized nature of **17**, falls in line with the other systems. For the six cyclometalated complexes reported in Table 3, a second oxidation band is observed at 1.13–1.36 V and is tentatively assigned to the removal of an electron from the carbanionic ligand.

The reductions are ligand based and represent the addition of an electron to a ligand π^* orbital.¹² In this regard, the

cyclometalated complexes are again quite consistent. The complexes of 2-phenylphen and its bridged derivatives all reduce at essentially the same potential (-1.57, -1.58 V). The more delocalized naphthalene system $[\text{Ru}(\text{tpy})(\mathbf{10b})]^+$ reduced more readily at -1.49 V, and $[\text{Ru}(\text{tpy})(\mathbf{17})]^+$ is the easiest to reduce at -1.33 V. The N5Cl complexes reduce more easily than their cyclometalated counterparts by 0.07–0.14 V, which is consistent with the carbanionic nature of the cyclometalated ligand. It is a little difficult to understand why the N5Cl complexes of the anthracenyl and pyrenyl systems are more difficult to reduce than their phenyl and naphthyl counterparts.

Conclusions

A variety of 2-aryl substituted derivatives of quinoline and 1,10-phenanthroline have been prepared and their possible complexation with Ru(II) has been examined. Of the six quinoline derivatives, only the 1,3-di-(2'-quinolinyl)benzene (**9H**) was found to undergo cyclometalation with $[\text{Ru}(\text{tpy})\text{Cl}_3]$. None of the potential bidentate cyclometalators reacted with $[\text{Ru}(\text{bpy})_2\text{Cl}_2]$. In contrast, all the 2-arylphen derivatives formed complexes with $[\text{Ru}(\text{tpy})\text{Cl}_3]$. Cyclometalation was observed when the incoming ligand was planar or could readily adopt a planar conformation. The more accessible nature of the central metal atom may account for the greater reactivity found with the tpy reagent, although the increased electrophilicity of Ru(III) may also play a role. The geometry of the N5Cl complexes, as best evidenced by $[\text{Ru}(\text{tpy})(\mathbf{13H})\text{Cl}]^+$, favors π stacking between the 2-aryl group and the tpy ligand over a less congested orientation which would hold these ligands further apart. The electrochemical reduction data does not support participation by low lying π^* states. In the N5Cl complexes this may be due to reduced conjugation with the coordinated phen and for the cyclometalated systems because of the anionic nature of the carbon-bound moiety.

Experimental Section

Nuclear magnetic resonance spectra were recorded on a General Electric QE-300 spectrometer at 300 MHz for ¹H NMR and 75 MHz for ¹³C NMR. Chemical shifts are reported in parts per million downfield from Me₄Si. Electronic spectra were obtained on a Perkin-Elmer 330 spectrophotometer. Cyclic voltammograms were recorded using a BAS CV-27 voltammograph and a Houston Instruments Model 100 X-Y recorder according to a procedure which has been described previously.¹⁷ Mass spectra were obtained on a Hewlett-Packard 5989B mass spectrometer (59987A electrospray) using atmospheric pressure ionization at 160 °C for the complexes and atmospheric pressure chemical ionization at 300 °C for the ligands. All solvents were freshly distilled reagent grade, and all melting points are uncorrected. Elemental analyses were performed by National Chemical Consulting, Inc., P.O. Box 99, Tenafly, NJ 07670.

Literature procedures were followed for the preparation of 2-aminobenzaldehyde,¹⁸ 8-amino-7-quinolinecarbaldehyde,¹⁰ 1,3-diacetylpyrene,⁸ and $[\text{Ru}(\text{tpy})\text{Cl}_3]$.¹⁹

1-(2'-Quinolinyl)pyrene (3H). A mixture of 1-acetylpyrene (244 mg, 1.0 mmol), 2-aminobenzaldehyde (121 mg, 1.0 mmol), and KOH (80 mg) in absolute EtOH (20 mL) was refluxed for 12 h under Ar and cooled to 25 °C. The mixture was added to H₂O (30 mL) and then extracted with CH₂Cl₂ (75 mL) to give **3H** (170 mg, 50%) as a yellow solid, mp 143–147 °C: ¹H NMR (CDCl₃): δ 8.46 (d, 1H, J = 9.4 Hz), 8.37 (d, 1H, J = 8.6 Hz), 8.29 (dd, 2H, J = 7.9–11.0 Hz), 8.26 (d, 1H, J = 6.4 Hz), 8.18 (dd, 2H, J = 8.6–9.5 Hz), 8.14 (s, 2H), 8.10

(17) Gouille, V.; Thummel, R. P. *Inorg. Chem.* **1990**, *29*, 1767.

(18) Opie, J. W.; Smith, L. I. *Organic Syntheses*; Wiley and Sons: New York, 1955; Coll. Vol. III, p 56.

(19) Sullivan, B. P.; Calvert, J. M.; Meyer, T. J. *Inorg. Chem.* **1980**, *19*, 1404.

(16) Thummel, R. P.; Chirayil, S. *Inorg. Chim. Acta* **1988**, *154*, 77.

(d, 1H, $J = 9.4$ Hz), 8.03 (t, 1H, $J = 7.7$ Hz), 7.94 (d, 1H, $J = 8.0$ Hz), 7.88 (d, 1H, $J = 8.0$ Hz), 7.81 (t, 1H, $J = 7.8$ Hz), 7.64 (t, 1H, $J = 7.8$ Hz). ^{13}C NMR (CDCl_3): δ 159.6, 148.1, 136.2 (2C), 135.7, 131.5, 131.3, 130.8, 129.8, 129.6, 128.7, 128.1, 127.9, 127.7, 127.5 (2C), 127.3, 126.8, 126.6, 126.0, 125.3, 125.1, 124.8 (2C), 123.7.

1,3-Di-(2'-quinolinyl)pyrene (7H). A mixture of 1,3-diacetylpyrene (28.6 mg, 0.1 mmol), 2-aminobenzaldehyde (24 mg, 0.2 mmol), and KOH (100 mg) in absolute EtOH (5 mL) was refluxed for 12 h. The yellow precipitate was filtered, washed with EtOH (2×5 mL), and dried to give **7H** (32 mg, 72%), mp > 270 °C. ^1H NMR (CDCl_3): δ 8.59 (s, 1H, H_2), 8.47 (d, 2H, H_4 or 5 , $J = 9$ Hz), 8.37 (d, 2H, H_3 ' or $4'$, $J = 8.4$ Hz), 8.31 (d, 2H, H_8 , $J = 8.4$ Hz), 8.24 (d, 2H, H_6 , $J = 7.8$ Hz), 8.14 (d, 2H, H_4 or 5 , $J = 9.3$ Hz), 8.06 (t, 1H, H_7 , $J = 7.5$ Hz), 7.95 (2d, 4H, H_5 ' and H_4 or 5), 7.81 (td, 2H, H_7 , $J = 6.9$, 1.2 Hz), 7.63 (td, 2H, H_6 , $J = 7.5$, 0.6 Hz). ^{13}C NMR (CDCl_3): δ 159.2, 136.8, 135.0, 131.1, 130.2, 129.9, 129.4, 129.3, 129.2, 128.9, 127.7, 127.0, 126.9, 126.3, 125.8, 125.7, 124.9, 124.7, 124.1. MS: m/z 456 (100, M).

1,3-Di-(2'-quinolinyl)benzene (9H). A mixture of 1,3-diacetylbenzene (50 mg, 0.3 mmol), 2-aminobenzaldehyde (72 mg, 0.6 mmol), and KOH (200 mg) in absolute EtOH (10 mL) was refluxed for 24 h. The mixture was cooled to 25 °C, and H_2O (20 mL) was added. The aqueous phase was extracted with CH_2Cl_2 (3×15 mL). The organic phase was dried (MgSO_4) and the solvent evaporated to provide a residue which was recrystallized from ether/ CH_2Cl_2 (6:1) to give **9H** (56 mg, 56%) as yellow needles, mp 139–40 °C. ^1H NMR (CDCl_3): δ 8.97 (s, 1H, H_2), 8.31–8.23 (m, 6H), 8.04 (d, 2H, $J = 8.7$ Hz), 7.87 (d, 2H, H_5 , $J = 8.1$ Hz), 7.76 (td, 2H, $J = 8.1$, 1.2 Hz), 7.71 (t, 1H, H_5 , $J = 7.5$ Hz), 7.56 (td, 2H, H_6 , $J = 7.8$, 0.9 Hz). ^{13}C NMR (CDCl_3): δ 157.3, 148.4, 140.4, 137.0, 129.9, 129.8, 129.6, 128.7, 127.7, 127.4, 126.9, 126.5, 119.3. MS: m/z 332 (100, M).

3,1'-Dimethylene-2-(2'-pyrenyl)-1,10-phenanthroline (13H). A mixture of **11** (300 mg, 1.11 mmol), 8-amino-7-quinolinecarbaldehyde (191 mg, 1.11 mmol), and KOH (120 mg) in absolute EtOH (25 mL) was refluxed for 12 h under Ar and cooled to 25 °C. After the mixture was added to H_2O (30 mL), the product was filtered, washed with ethanol, and recrystallized from chloroform to give **13H** (406 mg, 90%) as a light brown solid, mp 270 °C. ^1H NMR (CDCl_3): δ 9.81 (s, 1H, H_4), 9.32 (d, 1H, H_9 , $J = 3.9$ Hz), 8.37 (t, 1H, H_7 , $J = 8.2$ Hz), 8.26 (d, 1H, H_7 , $J = 7.9$ Hz), 7.95–8.4 (m, 8H, ArH), 7.78 (AB quartet, 2H, $\text{H}_{5,6}$, $J = 7.9$ Hz), 7.66 (dd, 1H, H_8 , $J = 3.9$ –7.8 Hz), 3.78 (t, 2H, CH_2), 3.44 (t, 2H, CH_2). ^{13}C NMR (CDCl_3): δ 222.5, 151.0, 150.4, 136.5, 134.6, 133.6, 133.0, 132.8, 132.1, 131.4, 130.2, 129.2, 129.0, 128.7, 128.2, 127.7, 127.1, 126.5, 126.4, 126.3, 125.3, 124.9, 124.0, 123.4, 122.8, 29.1, 24.4. Anal. Calcd for $\text{C}_{30}\text{H}_{18}\text{N}_2 \cdot 0.6 \text{H}_2\text{O}$: C, 86.37; H, 4.61; N, 6.72. Found: C, 86.01; H, 4.62; N, 7.04.

3,1'-Dimethylene-2-(2'-pyrenyl)-quinoline (14H). Following the procedure described for **3H**, 9,10-dihydrobenzo[*a*]pyren-7(8H)-one (350 mg, 1.29 mmol) in absolute EtOH (25 mL) for 6 h under Ar. The light yellow residue was filtered, washed with ethanol, and dried to afford **14H** (384 mg, 84%), mp 220–223 °C. ^1H NMR (CDCl_3): δ 9.47 (s, 1H, H_4), 8.40 (d, 1H, H_8 , $J = 8.8$ Hz), 7.96–8.30 (m, 8H, ArH), 7.81 (d, 1H, H_5 , $J = 6.47$ Hz), 7.71 (t, 1H, H_6 , $J = 7.35$ Hz), 7.55 (m, 1H, H_7 , $J = 7.38$ Hz), 3.74 (t, 2H, CH_2), 3.37 (t, 2H, CH_2). ^{13}C NMR (CDCl_3): δ 154.3, 148.2, 133.9, 133.8 (2C), 132.1, 131.4, 130.8, 130.5, 129.7 (2C), 129.1, 128.7, 128.4, 128.2, 127.8, 127.2, 126.4, 125.9, 125.3, 125.1, 125.0, 123.4, 123.2 (2C), 29.0, 24.3. Anal. Calcd for $\text{C}_{27}\text{H}_{17}\text{N} \cdot 0.5 \text{H}_2\text{O}$: C, 89.01; H, 4.95; N, 3.85. Found: C, 88.64; H, 4.65; N, 3.63.

3,2'-Dimethylene-2-phenyl-1,10-phenanthroline (16aH). Following the procedure described for **9H**, 1-tetralone (146 mg, 1 mmol) was condensed with 8-amino-7-quinolinecarbaldehyde (172 mg, 1 mmol) in absolute EtOH (12 mL) for 18 h. The brown, oily residue was chromatographed on Al_2O_3 (30 g), eluting with EtOAc/hexane (1:1). The second fraction afforded **16aH** (232 mg, 82%) as a yellow solid, mp 151–153 °C. ^1H NMR (CDCl_3): δ 9.22 (dd, 1H, H_9 , $J = 4.5$, 1.8 Hz), 8.91 (d, 1H, H_3 ', $J = 7.8$ Hz), 8.20 (dd, 1H, H_7 , $J = 8.1$, 1.5 Hz), 7.97 (s, 1H, H_4), 7.70 (AB quartet, 2H, $\text{H}_{5,6}$), 7.59 (dd, 1H, H_8 , $J = 8.1$, 4.5 Hz), 7.44 (t, 1H, H_4 ', $J = 7.2$ Hz), 7.36 (td, 1H, H_5 ', $J = 7.2$, 0.9 Hz), 7.26 (m, 1H, H_6 '), 3.17 (t, 2H, CH_2), 3.02 (t, 2H, CH_2). ^{13}C

NMR (CDCl_3): δ 153.3, 150.2, 146.4, 145.0, 138.8, 136.0, 134.6, 134.4, 132.3, 129.6, 128.5, 128.1, 127.6, 127.3, 127.0, 126.2, 125.9, 122.4, 28.6, 28.1. MS: m/z 281 (100, M – 1).

3,2'-Trimethylene-2-phenyl-1,10-phenanthroline (16bH). Following the procedure described for **9H**, benzosuberone (179 mg, 1.12 mmol) was condensed with 8-amino-7-quinolinecarbaldehyde (192 mg, 1.12 mmol) in absolute EtOH (20 mL) for 18 h. The dark-orange, oily residue was chromatographed on Al_2O_3 (30 g), eluting with EtOAc/hexane (1:1). The second fraction afforded **16bH** (173 mg, 52%) as a yellow solid, mp 112–114 °C. ^1H NMR (CDCl_3): δ 9.20 (dd, 1H, H_9 , $J = 4.2$, 1.5 Hz), 8.24 (dd, 1H, H_7 , $J = 8.1$, 1.8 Hz), 8.10 (dd, 1H, H_3 ', $J = 7.5$, 1.2 Hz), 8.07 (s, 1H, H_4), 7.79 (AB quartet, 2H, $\text{H}_{5,6}$), 7.61 (dd, 1H, H_8 , $J = 8.1$, 4.5 Hz), 7.45 (td, 1H, H_4 ', $J = 7.5$, 1.2 Hz), 7.38 (td, 1H, H_5 ', $J = 7.5$, 1.5 Hz), 7.26 (dd, 1H, H_6 ', $J = 8.4$, 1.2 Hz), 2.76 (t, 2H, CH_2), 2.59 (t, 2H, CH_2), 2.28 (quintet, 2H, CH_2). ^{13}C NMR (CDCl_3): δ 150.5, 146.8, 145.0, 140.6, 139.3, 136.2, 135.5, 135.2, 130.2, 129.3, 129.2, 128.7, 128.2, 128.1, 127.2, 126.4, 126.3, 122.7, 32.4, 31.0, 30.8. MS: m/z 295 (100, M – 1).

3,2'-Naphtho-[1,2-*b*]-1,10-phenanthroline (17H). A mixture of **16aH** (185 mg, 0.65 mmol) and 10% Pd/C (100 mg) in nitrobenzene (5 g) was refluxed for 24 h. The reaction mixture was cooled to 25 °C, and 10% Pd/C (100 mg) in nitrobenzene (2 g) was added. The reflux was continued for another 24 h. After cooling, the Pd/C was removed by filtration through Celite and washed with CH_2Cl_2 (20 mL). The CH_2Cl_2 was evaporated, and the nitrobenzene solution was chromatographed on Al_2O_3 (30 g), eluting first with CH_2Cl_2 /hexane (1:1), to remove all the nitrobenzene, and then with CHCl_3 , to provide a brown solid which was washed with Et₂O/hexane (1:1) to give **17H** (108 mg, 59%) as a beige solid, mp 200–201 °C. ^1H NMR (CDCl_3): δ 9.95 (d, 1H, H_8 ', $J = 7.8$ Hz), 9.34 (dd, 1H, H_9 ', $J = 2.7$, 0.9 Hz), 8.69 (s, 1H, H_4), 8.31 (d, 1H, H_7 ', $J = 7.8$ Hz), 7.96–7.69 (m, 8H). ^{13}C NMR (CDCl_3): δ 149.9, 149.8, 147.5, 146.2, 135.6, 135.3, 134.1, 129.3, 129.0, 127.9, 127.7, 127.5, 127.4, 126.8, 126.7, 126.4, 126.0, 125.3, 123.4. MS: m/z 280 (100, M).

[Ru(tpy)(9)](PF₆). A mixture of $[\text{Ru}(\text{tpy})\text{Cl}_3]$ (44 mg, 0.1 mmol), **9H** (33 mg, 0.1 mmol), and Et₃N (3 drops) in EtOH/ H_2O (3:1, 12 mL) was refluxed for 12 h. After cooling and filtering, NH_4PF_6 (16.3 mg, 0.1 mmol) was added to the filtrate, and the solvent was evaporated to dryness. The resulting mauve residue was chromatographed on Al_2O_3 (30 g), eluting with CH_3CN /toluene (1:1), to provide the complex as purple crystals (25 mg, 31%), mp > 270 °C. ^1H NMR (CD_3CN): δ 8.93 (d, 2H, H_e , $J = 8.1$ Hz), 8.57 (d, 2H, H_4 , $J = 7.5$ Hz), 8.53 (t, 1H, H_f , $J = 8.1$ Hz), 8.41 (d, 2H, H_4 ', $J = 8.7$ Hz), 8.33 (d, 2H, H_4 , $J = 8.1$ Hz), 8.11 (d, 2H, H_3 ', $J = 8.7$ Hz), 7.65 (m, 3H, $\text{H}_{5,5'}$), 7.53 (dd, 2H, H_c , $J = 7.8$, 1.2 Hz), 7.42 (t, 2H, H_6 ', $J = 7.5$ Hz), 7.16 (d, 2H, H_a , $J = 5.4$ Hz), 7.00 (td, 2H, H_7 ', $J = 8.5$, 1.5 Hz), 6.84 (td, 2H, H_b , $J = 6.6$, 0.9 Hz), 6.53 (d, 2H, H_8 ', $J = 8.7$ Hz). MS: m/z 664 (100, M – PF₆).

[Ru(tpy)(10a)](PF₆) and [Ru(tpy)(10aH)Cl](PF₆). Following the procedure described for $[\text{Ru}(\text{tpy})(9)](\text{PF}_6)$, **10aH** (64 mg, 0.25 mmol) was treated with $[\text{Ru}(\text{tpy})\text{Cl}_3]$ (110 mg, 0.25 mmol) and refluxed for 5 h. The first fraction gave 72 mg (39%) of $[\text{Ru}(\text{tpy})(10a)](\text{PF}_6)$ as a purple solid, mp > 270 °C. ^1H NMR (CDCl_3): δ 8.60 (dd, 2H, H_e , $J = 8.1$, 3.0 Hz), 8.53 (AB quartet, 2H, $\text{H}_{5,6}$), 8.40 (d, 2H, H_a , $J = 8.1$ Hz), 8.31 (d, 1H, H_7 , $J = 8.1$ Hz), 8.23 (d, 1H, H_4 , $J = 9.0$ Hz), 8.08 (t, 1H, H_f , $J = 8.1$ Hz), 8.04 (d, 1H, H_3 , $J = 9.3$ Hz), 7.95 (d, 1H, H_6 ', $J = 7.5$ Hz), 7.84 (d, 1H, H_9 , $J = 5.4$ Hz), 7.73 (t, 2H, H_b , $J = 7.5$ Hz), 7.31 (dd, 1H, H_8 , $J = 8.4$, 5.1 Hz), 7.24 (d, 2H, H_d , $J = 4.8$ Hz), 6.90 (td, 2H, H_c , $J = 6.6$, 1.5 Hz), 6.76 (td, 1H, H_5 ', $J = 7.2$, 2.7 Hz), 6.54 (td, 1H, H_4 ', $J = 7.2$, 1.2 Hz), 5.80 (d, 1H, H_3 ', $J = 7.2$ Hz). The second fraction afforded $[\text{Ru}(\text{tpy})(10a\text{H})\text{Cl}](\text{PF}_6)$ as a red solid (22.5 mg, 12%). ^1H NMR (CDCl_3): δ 10.46 (dd, 1H, H_9 , $J = 6.3$, 0.9 Hz), 8.82 (d, 1H, H_7 , $J = 9.3$ Hz), 8.39 (d, 1H, H_5 or 6 , $J = 8.7$ Hz), 8.27 (d, 1H, H_4 , $J = 8.4$ Hz), 8.24–8.18 (m, 4H, $\text{H}_{8,d}$ and H_5 or 6), 7.99 (d, 2H, H_e , $J = 8.1$ Hz), 7.85 (td, 2H, H_c , $J = 7.8$, 1.5 Hz), 7.68 (t, 1H, H_f , $J = 8.1$ Hz), 7.39 (d, 2H, H_a , $J = 5.4$ Hz), 7.21–7.09 (m, 4H, $\text{H}_{3,4,b}$), 6.94 (td, 2H, $\text{H}_{3,5'}$, $J = 7.5$, 1.5 Hz), 6.11 (d, 2H, $\text{H}_{2,6'}$, $J = 6.9$

(20) The tpy protons are designated as follows: $\text{H}_a = \text{H}_6$, $\text{H}_b = \text{H}_5$, $\text{H}_c = \text{H}_4$, $\text{H}_d = \text{H}_3$, $\text{H}_e = \text{H}_3'$, and $\text{H}_f = \text{H}_4'$.

H_z). Anal. Calcd for C₃₃H₂₃N₅ClRuPF₆ · 0.5 H₂O: C, 50.80; H, 3.08; N, 8.98. Found: C, 50.68; H, 2.45; N, 8.81.

[Ru(tpy)(10b)Cl](PF₆) and [Ru(tpy)(10bH)Cl](PF₆). Following the procedure described for [Ru(tpy)(9)](PF₆), **10bH** (30 mg, 0.1 mmol) was treated with [Ru(tpy)Cl₃] (44 mg, 0.1 mmol) and refluxed for 5 h. The first fraction afforded [Ru(tpy)(10b)](PF₆) as a purple solid (11.8 mg, 15%), mp > 270 °C, which showed a mixture of two isomers by ¹H NMR (CD₃CN): δ 8.8–6.8 (complex pattern of overlapping peaks accounting for 50 nonequivalent H), 6.42 (d, H_g), 6.15 (s, H₄). MS: 640 *m/z* (100, M + 1 – PF₆). The second fraction afforded [Ru(tpy)(10bH)Cl](PF₆) as a red solid (28.6 mg, 35%), mp > 270 °C, ¹H NMR (CD₃CN): δ 10.46 (dd, 1H, *J* = 4.2, 1.2 Hz), 8.83 (dd, 1H, *J* = 8.1, 1.2 Hz), 8.42–8.34 (m, 2H), 8.21–8.19 (m, 3H), 8.00 (d, 1H, *J* = 8.1 Hz), 7.89–7.84 (m, 3H), 7.72 (d, 1H, *J* = 8.1 Hz), 7.65 (m, 2H), 7.49–7.37 (m, 4H), 7.28–7.22 (m, 2H), 7.16–7.09 (m, 2H), 6.96 (t, 1H, *J* = 7.8 Hz), 6.5 (s, 1H), 6.27 (dd, 1H, *J* = 8.1 Hz). MS: *m/z* 676 (100, M + 1 – PF₆). Anal. Calcd for C₃₇H₂₅N₅ClRuPF₆: C, 54.11; H, 3.04; N, 8.53. Found: C, 54.16; H, 2.89; N, 8.30.

[Ru(tpy)(10cH)Cl](PF₆). Following the procedure described for [Ru(tpy)(9)](PF₆), **10cH** (35.6 mg, 0.1 mmol) was treated with [Ru(tpy)Cl₃] (44 mg, 0.1 mmol) and refluxed for 5 h to give 41 mg (47%) of the complex as a red solid, mp > 270 °C. ¹H NMR (CD₃CN): δ 10.42 (dd, 1H, *J* = 5.4, 1.2 Hz), 8.88 (dd, 1H, *J* = 8.4, 1.2 Hz), 8.45–8.40 (m, 3H), 8.31 (d, 1H, *J* = 8.7 Hz), 8.17 (m, 2H), 8.10 (d, 1H, *J* = 8.4 Hz), 7.94–7.83 (m, 3H), 7.70 (d, 1H, *J* = 5.4 Hz), 7.57 (td, 1H, *J* = 8.4, 3.3 Hz), 7.38 (t, 1H, *J* = 9 Hz), 7.32–7.26 (m, 3H), 7.19 (td, 1H, *J* = 6.9, 0.9 Hz), 7.11–7.03 (m, 3H), 6.91 (td, 1H, *J* = 7.2, 1.5 Hz), 6.77–6.68 (m, 2H), 6.59 (s, 1H), 5.90 (dd, 1H, *J* = 6.6, 0.6 Hz). MS: *m/z* 726 (100, M + 1 – PF₆).

[Ru(tpy)(10dH)Cl](PF₆). Following the procedure described for [Ru(tpy)(9)](PF₆), **10dH** (76 mg, 0.2 mmol) was treated with [Ru(tpy)Cl₃] (88 mg, 0.2 mmol) and refluxed for 5.5 h to afford 60 mg (32%) of the complex as a red–brown solid, mp > 270 °C. ¹H NMR (CD₃CN): δ 10.41 (d, 1H, *J* = 4.8 Hz), 8.85 (d, 1H, *J* = 9.0 Hz), 8.41 (m, 2H), 8.31–8.09 (m, 6H), 7.91 (t, 1H, *J* = 6.9 Hz), 7.72 (d, 1H, *J* = 7.8 Hz), 7.64 (d, 1H, *J* = 5.1 Hz), 7.57 (t, 1H, *J* = 7.8 Hz), 7.39 (m, 2H), 7.27–7.06 (m, 6H), 7.04 (t, 1H, *J* = 6.6 Hz), 6.5 (d, 1H, *J* = 7.5 Hz), 6.39–6.23 (m, 3H). MS: *m/z* 750 (100, M + 1 – PF₆).

[Ru(tpy)(13)](PF₆) and [Ru(tpy)(13H)Cl](PF₆). A mixture of [Ru(tpy)Cl₃] (54 mg, 0.123 mmol) and **13H** (50 mg, 0.123 mmol) in EtOH/H₂O (3:1, 12 mL) was refluxed for 12 h. After cooling, NH₄PF₆ was added, and the solvent was evaporated to dryness. The resulting mauve residue was chromatographed on Al₂O₃ (40 g), eluting with CH₂Cl₂/CH₃CN (9:1). The first fraction afforded [Ru(13)(tpy)](PF₆) as a purple solid (30 mg, 46%), mp > 270 °C. ¹H NMR (CD₃CN): δ 8.74 (d, 2H, H_e, *J* = 7.31 Hz), 8.39–8.35 (m, 3H), 8.30–8.19 (m, 4H), 7.98 (d, 1H, *J* = 9.14 Hz), 7.88–7.71 (m, 4H), 7.59 (d, 2H, *J* = 7.31 Hz), 7.40–7.24 (m, 5H), 6.77 (t, 2H, *J* = 7.31 Hz), 6.44 (d, 1H, *J* = 9.14 Hz), 4.01 (t, 2H, CH₂), 3.82 (t, 2H, CH₂). The second fraction gave [Ru(13H)(tpy)Cl](PF₆) as a dark red solid (25 mg, 18%), mp > 270 °C. ¹H NMR (CD₃CN): δ 10.28 (d, 1H, H₉, *J* = 5.29 Hz), 8.84 (d, 1H, H₇, *J* = 7.76 Hz), 8.58 (d, 1H, H_d, *J* = 6.35 Hz), 8.32 (d, 1H, H_a, *J* = 7.05 Hz), 8.32–8.25 (m, 5H), 8.19–8.11 (m, 2H), 8.04–8.00 (m, 3H), 7.87 (d, 1H, H_e or _g, *J* = 7.05 Hz), 7.02 (d, 1H, *J* = 6.35 Hz), 6.92 (d, 1H, *J* = 7.76 Hz), 6.78 (t, 1H, *J* = 7.41 Hz), 6.61 (s, 1H, H₃), 6.56 (d, 1H, *J* = 5.29 Hz), 6.14 (t, 1H, *J* = 7.41 Hz), 3.62 (t, 2H, CH₂), 2.83 (t, 2H, CH₂). The experiment was repeated using [Ru(tpy-*d*₁₁-Cl₃)] and analogous results were obtained. A crystal of the N5Cl complex was used for X-ray analysis.

[Ru(tpy)(16a)](PF₆) and [Ru(tpy)(16aH)Cl](PF₆). Following the procedure described for [Ru(tpy)(9)](PF₆), **16aH** (28.2 mg, 0.1 mmol) was treated with [Ru(tpy)Cl₃] (44 mg, 0.1 mmol) and refluxed for 18 h. The first fraction gave [Ru(16a)(tpy)](PF₆) as a purple solid (31 mg, 40%), mp > 270 °C. ¹H NMR (CD₃CN):²⁰ δ 8.60 (d, 2H, H_e, *J* = 7.8 Hz), 8.40 (d, 2H, H_d, *J* = 8.1 Hz), 8.30 (dd, 1H, H₇, *J* = 8.1, 0.9 Hz), 8.23 (s, 1H, H₄), 8.19 (d, 1H, H₅ or ₆, *J* = 9.0 Hz), 8.06 (t, 1H, H_f, *J* = 8.1 Hz), 7.97 (d, 1H, H₅ or ₆, *J* = 9.0 Hz), 7.86 (dd, 1H, H₉, *J* = 5.1, 0.9 Hz), 7.70 (td, 2H, H_c, *J* = 8.1, 1.2 Hz), 7.29–7.25 (d and dd, 3H, H_{8,a}), 6.91 (td, 2H, H_b, *J* = 6.9, 0.9 Hz), 6.54–6.44 (d and t, 2H, H₃, ₄), 5.61 (d, 1H, H₅, *J* = 6.9 Hz), 3.45 (t, 2H, CH₂), 3.17 (t, 2H, CH₂). The second fraction afforded [Ru(tpy)(16aH)Cl](PF₆) as a red solid

(38 mg, 48%), mp > 270 °C. ¹H NMR (–40 °C) (CD₃CN): δ 10.20 (d, 1H, H₉, *J* = 5.1 Hz), 8.82 (d, 1H), 8.49 (d, 1H), 8.43 (d, 1H), 8.23 (m, 2H), 8.08 (d, 1H), 8.03 (t, 1H), 7.97–7.89 (m, 3H), 7.83 (d, 1H), 7.59 (t, 1H), 7.50 (t, 1H), 7.43 (t, 1H), 6.98 (m, 2H), 6.73 (t, 1H), 6.56 (t, 1H), 6.53 (d, 1H), 5.67 (d, 1H, H₈, *J* = 7.5 Hz), 2.49 (m, 1H), 2.22 (m, 1H), 1.63 (m, 3H), 1.08 (m, 1H). Anal. Calcd for C₃₅H₂₅N₅ClRuPF₆ · 0.5 C₇H₈: C, 54.83; H, 3.44; N, 8.31. Found: C, 54.38; H, 3.19; N, 8.27.

[Ru(tpy)(16b)](PF₆) and [Ru(tpy)(16bH)Cl](PF₆). Following the procedure described for [Ru(tpy)(9)](PF₆), **16bH** (59.2 mg, 0.2 mmol) was treated with [Ru(tpy)Cl₃] (88 mg, 0.2 mmol) and refluxed for 18 h. The first fraction afforded [Ru(tpy)(16b)](PF₆) as a purple solid (9.5 mg, 6%), mp > 270 °C. ¹H NMR (CD₃CN):²⁰ δ 8.63 (d, 2H, H_e, *J* = 8.1 Hz), 8.40 (d, 2H, H_d, *J* = 8.1 Hz), 8.30 (s, 1H, H₄), 8.26 (d, 1H, H₇, *J* = 8.1 Hz), 8.13 (d, 1H, H₅ or ₆, *J* = 9.0 Hz), 8.07 (t, 1H, H_f, *J* = 8.1 Hz), 7.98 (d, 1H, H₅ or ₆, *J* = 9.0 Hz), 7.68 (d and t, 3H, H₉, H_c), 7.23 (d and dd, 3H, H₈, H_a), 6.87 (t, 2H, H_b, *J* = 6.6 Hz), 6.51 (d, 1H, H₃, *J* = 6.9 Hz), 6.29 (t, 1H, H₄, *J* = 7.2 Hz), 5.59 (d, 1H, H₅, *J* = 6.9 Hz), 3.57 (t, 2H, CH₂), 3.21 (t, 2H, CH₂), 2.27 (m, 2H, CH₂). The second fraction gave [Ru(tpy)(16bH)Cl](PF₆) as a red solid (55.8 mg, 34%), mp > 270 °C. ¹H NMR (CD₃CN): δ 10.36 (d, 1H, H₉, *J* = 5.4 Hz), 8.82 (dd, 1H), 8.32 (m, 2H), 8.17 (dd, 1H), 8.09–8.06 (m, 3H), 8.04 (s, 1H), 7.99–7.93 (m, 3H), 7.68 (td, 1H), 7.61 (t, 1H), 7.34 (td, 1H), 7.12 (td, 1H), 6.90 (m, 2H), 6.79 (d, 1H), 6.67 (td, 1H), 5.45 (dd, 1H, H₆, *J* = 7.2, 0.9 Hz), 2.49 (m, 1H), 2.22 (m, 1H), 1.63 (m, 3H), 1.08 (m, 1H). Anal. Calcd for C₃₆H₂₇N₅ClRuPF₆ · 0.75 H₂O: C, 52.43; H, 3.46; N, 8.50. Found: C, 52.49; H, 3.36; N, 8.37.

[Ru(tpy)(17)](PF₆). Following the procedure described for [Ru(tpy)(9)](PF₆), **17H** (28 mg, 0.1 mmol) was treated with [Ru(tpy)Cl₃] (44 mg, 0.1 mmol) and refluxed for 4.5 h to give 43 mg (57%) of [Ru(tpy)(17)](PF₆), mp > 270 °C. ¹H NMR (CD₃CN):^{20,21} δ 8.93 (s, 1H, H₇), 8.65 (d, 2H, H_e, *J* = 8.1 Hz), 8.43–8.36 (m, 4H, H₄, H₈ or ₉ and H_a), 8.13 (t, 1H, H_f, *J* = 8.1 Hz), 8.11–8.05 (2d, 2H, H₈ or ₉ and H₅ or ₆), 8.00 (dd, 1H, H₂, *J* = 4.2, 0.9 Hz), 7.90 (d, 1H, H₅ or ₆, *J* = 9 Hz), 7.64 (td, 2H, H_c, *J* = 8.4, 1.2 Hz), 7.37 (dd, 1H, H₃, *J* = 8.1, 4.8 Hz), 7.28 (d, 1H, H₁₀, *J* = 8.1 Hz), 7.07 (d, 2H, H_a, *J* = 5.1 Hz), 6.93 (t, 1H, H₁₁, *J* = 7.5 Hz), 6.74 (td, 2H, H_b, *J* = 4.8, 1.5 Hz), 6.15 (d, 1H, H₁₂, *J* = 7.2 Hz). MS: *m/z* 613 (100, M – PF₆). Anal. Calcd for C₃₅H₂₂N₅RuPF₆: C, 55.40; H, 2.90; N, 9.23. Found: C, 55.00; H, 2.91; N, 8.93.

X-ray Determinations. [Ru(tpy)(13)](PF₆). A dark red column having approximate dimensions 0.50 × 0.15 × 0.10 mm was mounted in a random orientation on a Nicolet R3m/V automatic diffractometer. The sample was placed in a steam of dry nitrogen gas at –50 °C, and the radiation used was Mo K monochromatized by a highly ordered graphite crystal. Final cell constants, and other information pertinent to data collection and refinement, are listed in Table 4. The Laue symmetry was determined to be 2/m, and from the systematic absences noted, the space group was shown unambiguously to be *P*2₁/*n*. Intensities were measured using the ω scan technique, with the scan rate depending on the count obtained in rapid prescans of each reflection. Two standard reflections were monitored after every 2 h of every 100 data collected, and these showed no significant variation. During data reduction, Lorentz and polarization corrections were applied, however, no correction for absorption was made due to the small absorption coefficient.

The structure was solved by the SHELXTL direct methods program, which revealed the positions of most of the nonhydrogen atoms in the molecule. Remaining atoms were located in subsequent difference Fourier syntheses. The usual sequence of isotropic and anisotropic refinement was followed, after which all the hydrogens were entered in ideal calculated positions and constrained to riding motion, with a single variable isotropic temperature factor for all of them. After all shift/esd ratios were less than 0.1, convergence was reached at the agreement factors listed in Table 4. No unusually high correlations were noted between any of the variables in the last cycle of full-matrix least-

(21) The NMR atom numbering scheme designates N10 as H₁, and each successive nonbridgehead carbon atom on the periphery of the molecule is then numbered sequentially proceeding away from the bay region of the molecule.

Table 4. Data Collection and Processing Parameters for [Ru(tpy)(**13**)](PF₆) and [Ru(tpy-*d*₁₁)(**13H**)(Cl)](PF₆)

	[Ru(tpy)(13)](PF ₆)	[Ru(tpy- <i>d</i> ₁₁)(13H)(Cl)](PF ₆) + 1.5 C ₆ H ₆ + CH ₃ CN
chemical formula	C ₄₅ H ₂₈ F ₆ N ₅ PRu	C ₄₅ H ₁₈ D ₁₁ ClF ₆ N ₅ PRu-C ₁₁ H ₁₂ N
space group	<i>P</i> 2 ₁ / <i>n</i> (monoclinic)	<i>P</i> -1 (triclinic)
<i>a</i> , Å	28.1102(11)	11.7235(10)
<i>b</i> , Å	8.4638(3)	14.5306(12)
<i>c</i> , Å	31.2908(12)	14.5725(12)
α , deg	90	75.536(1)
β , deg	107.505(1)	85.511(2)
γ , deg	90	79.812(1)
<i>V</i> , Å ³	7099.9(5)	2364.3(3)
formula weight, g/mol	884.76	1090.50
formula units per cell, <i>Z</i>	8	2
density, g/cm ³	1.655	1.532
absorption coefficient, cm ⁻¹	$\mu = 5.62$	$\mu = 4.93$
temp, °C	-50	-50
λ , radiation (Mo K), Å	0.71073	0.71073
number of refined parameters	581	1045
number of observables	5322	8013
$R_1 = \sum F_o - F_c / \sum F_o $	0.0303	0.0581
$^a wR_2 = [\sum w(F_o^2 - F_c^2)^2 / \sum w(F_o^2)^2]^{1/2}$	0.0728	0.1538

^a For [Ru(tpy)(**13**)](PF₆), $w = [\sigma(F_o)^2 + (0.0333P)^2 + (11.656P)]^{-1}$, and for [Ru(tpy-*d*₁₁)(**13H**)(Cl)](PF₆), $w = [\sigma(F_o)^2 + (0.1134P)^2 + (4456P)]^{-1}$, where $P = (F_o^2 + 2F_c^2)/3$.

squares refinement, and the final difference density map showed a maximum peak of about 0.78 e/Å³. All calculations were made using Bruker's SHELXS-97 (Sheldrick, 1997) series of crystallographic programs.²²

[Ru(tpy)(13H**)(Cl)](PF₆)**. All measurements were made with a Siemens SMART platform diffractometer equipped with a 1K CCD area detector. A hemisphere of data (1271 frames at 5 cm detector distance) was collected using a narrow-frame method, with scan widths of 0.30° in ω and an exposure time of 30 s/frame. The first 50 frames were remeasured at the end of data collection to monitor instrument and crystal stability, and the maximum correction on *I* was < 1%. The data were integrated using the Siemens SAINT program, with the intensities corrected for Lorentz factor, polarization, air absorption, and absorption due to variation in the path length through the detector faceplate. A ψ scan absorption correction was applied based on the entire data set. Redundant reflections were averaged. Final cell constants were refined using 6869 reflections having $I > 10\sigma(I)$, and these, along with other information pertinent to data collection and refinement, are

listed in Table 4. The Laue symmetry was determined to be -1 , and the space group was shown to be either *P*1 or *P*-1. The anion was found to be massively disordered, and the three major orientations were refined as individual rigid bodies. One of the benzene solvent molecules was found to be disordered 50:50 over two staggered orientations, and these were also entered as ideal rigid bodies. One site in the lattice was found to be occupied 50% of the time by benzene and 50% of the time by a pair of acetonitrile molecules. A combination of rigid bodies and distance constraints was used to model this area.

Acknowledgment. We would like to thank the Robert A. Welch Foundation (E-621) and the National Science Foundation (CHE-9714998) for financial support of this work. We would also like to thank Dr. James Korp for assistance with the X-ray analysis, and one of the referees for helpful comments.

Supporting Information Available: X-ray crystallographic files for [Ru(tpy)(**13**)](PF₆) and [Ru(tpy-*d*₁₁)(**13H**)(Cl)](PF₆) in CIF format. This material is available free of charge via the Internet at <http://pubs.acs.org>.

(22) Sheldrick, G. M. In *Crystallographic Computing 3*; Sheldrick, G. M., Kruger, C., Goddard, R., Eds.; Oxford University Press: Oxford, U. K., 1985, pp 175-189.